NASA Contractor Report 189686

ICASE Report No. 92-36

ICASE

ADAPTIVE MESH STRATEGIES FOR THE
SPECTRAL ELEMENT METHOD

Catherine Mavriplis

NASA

National Aeronautics and
Space Administration

Langley Research Center
Hampton, Virginia 23665-5225

ADAPTIVE MESH STRATEGIES
FOR THE SPECTRAL ELEMENT METHOD [1]

Catherine Mavriplis

CMEE Academic Center T713
The George Washington University
Washington, DC 20052 USA

ABSTRACT

An adaptive spectral element method has been developed for the efficient solution of time dependent partial differential equations. Adaptive mesh strategies that include resolution refinement and coarsening by three different methods are illustrated on solutions to the one-dimensional viscous Burgers equation and the two-dimensional Navier-Stokes equations for driven flow in a cavity. Sharp gradients, singularities and regions of poor resolution are resolved optimally as they develop in time using error estimators which indicate the choice of refinement to be used. The adaptive formulation presents significant increases in efficiency, flexibility and general capabilities for high order spectral methods.

i

1. Introduction

The adaptive formulation of the spectral element method is aimed at increasing the flexibility and range of capabilities of high order spectral methods in general. While spectral methods provide highly accurate solutions to partial differential equations governing complex physical phenomena, they have been limited to idealized research problems due to their lack of geometric flexibility [e.g. 1,2]. Further, while they offer exponential convergence for infinitely smooth solutions [3], they have not been useful for problems presenting singularities or thin layers. The spectral element method [4] was developed to increase the geometrical flexibility of high order spectral methods. In this paper, we present an adaptive spectral element method which automatically allocates resolution where it is most needed in an optimal fashion. Singularities and thin internal and boundary layers are resolved efficiently as they develop in time. Coupled with advances in computer power, the development of an adaptive spectral element method presents a tremendous opportunity for high accuracy solutions to "real" engineering problems, by reducing the needed computer resources, in terms of storage and cpu time, by several orders of magnitude.

Previous work in nonconforming discretizations [5] and error estimators [6] for the spectral element method constituted a first step towards the adaptive formulation. Nonconforming discretizations, which allow arbitrary element matchup in the grid, account for a substantial savings in resolution over the structured conforming grid spectral element method. A further gain in efficiency can be achieved by automating the resolution allocation process. For this purpose, error estimators were developed to indicate local elemental error values as well as quality of resolution, as measured by decay rates in the solution spectrum. Some less theoretical yet very practical issues of an adaptive method are investigated here. A summary of adaptive mesh strategies is presented.

Adaptive mesh capabilities rely on a consistent and efficient rule-based system for refining, coarsening and reconstructing a mesh. The components of this rule-based system are determined and illustrated by solving the viscous Burgers equation in one dimension. The relative merits of changing element size, element position, the number of elements and the order of polynomials locally as well as globally is explored. These adaptive refinement options are selected based on global mesh optimization criteria as well as local elemental error estimators. The criteria provide the necessary constraints on the overall mesh refinement process to ensure global efficiency and optimization.

Adaptive mesh capabilities are illustrated by two examples. The solution of the one-dimensional viscous Burgers equation illustrates the adaptive procedure in the presence of sharp (low viscosity) and weak (high viscosity) gradients. This newly flexible formulation for spectral methods in general, will allow physical problems with sharp gradients, such as compressible flows with shocks, to be treated automatically, irrespective of the physical application. A two-dimensional fluid flow simulation illustrates the ability of the adaptive procedure to treat singularities. The full incompressible Navier-Stokes equations are solved for a highly accurate simulation of laminar flow in a geometry presenting functional singularities.

2. Formulation

In this section the components of the adaptive formulation are described. Together, they form a rule-based system designed to produce an optimally efficient and accurate solution to

any time-dependent solution of physical phenomena governed by partial differential equations. The adaptive formulation relies on an efficient and accurate estimate of the numerical error incurred by discretization. The error estimators are the subject of a detailed paper [6]. They will be reviewed briefly here.

2.1 Error Estimator

Single mesh a posteriori error estimators were developed to estimate the error and indicate the quality of resolution on each element. They rely on the calculation and extrapolation of the spectrum of the solution on each element to estimate the error and to predict convergence as well. Since the spectral element method offers several refinement options, namely increasing the polynomial order or increasing the number of elements, it is important that the error estimator be able to distinguish which of these refinement options is optimal. The decay rate of the spectrum offers information on the quality of the solution. A low decay rate is indicative of poor resolution or the presence of a singularity. A high decay rate, on the other hand, indicates that the solution is well-resolved. This information is used in the refinement process.

The error estimate ϵ_{est} used is given in terms of the spectrum a_n of the numerical solution u_h, defined by the elemental spectral discretization:

$$u_h^k(r) = \sum_{n=0}^{N} a_n^k P_n(r) \tag{1}$$

where P_n is the nth order Legendre polynomial, and N is the discretization order on element k. r is the local elemental spatial coordinate. The error estimate is calculated as

$$\epsilon_{est} = \left(\frac{a_N^2}{\frac{2N+1}{2}} + \int_{N+1}^{\infty} \frac{(a(n))^2}{\frac{2n+1}{2}} dn \right)^{\frac{1}{2}} \tag{2}$$

This is an approximation to the $\mathcal{L}^2$ error. The error in the $\mathcal{H}^1$ norm may be calculated analogously. The integral in Equation (2) represents the extrapolation of the spectrum to infinity, a measure of the truncation error. The function $a(n)$ is a least squares best fit of the last four points of the spectrum to an exponential decay:

$$a(n) = ce^{-\sigma}. \tag{3}$$

The decay rate σ indicates poor resolution for $\sigma < 1$ and good resolution for $\sigma > 1$. In the adaptive process, this information is used to refine by increasing the number of elements and increasing the order of the polynomial respectively. The value ϵ_{est} on each element is used to decide whether to adapt or not. In practice, we find that these error estimators are very robust and quite accurate as shown in [6] and in the following examples.

2.2 Refinement Criteria

The refinement decision is based on several criteria. The first and most effective is to compare elemental error estimators to a globally acceptable level of error, set once for the whole run. The elements with errors over the acceptable level are marked for refinement. The elemental error estimators are also compared in a relative manner to neighbouring elements in

2

order to determine which element has the greatest need for increased resolution. This criterion is implemented for situations where resolution is limited and only certain elements may be refined. It is also used in the no-cost "refinement" option which simply changes element sizes without incurring any increase in resolution. Limits and tolerances are imposed at every step of the decision process. At each refinement step the minimum and maximum error are calculated. If they are both below the acceptable level, no refinement is needed and the calculation proceeds. When comparing error estimates between elements, there must be a substantial difference in error, usually a factor of two or more, to be able to distinguish which element needs more resolution. Further, if any element has a substantially higher error than the minimum error, usually a factor of five or more, then it is also marked for refinement. There are also situations where one cannot refine. For these we implement limits that prevent refinement from occurring. If maximum values of N, the order of the polynomial, K, the number of elements, or NTOTAL, the total number of degrees of freedom, are reached refinement is prohibited. Similarly, if minimum values of element size or time step size, which decreases with resolution in order to satisfy stability conditions, are reached refinement is prohibited.

The decision to refine by adding elements or increasing the order of the polynomial is straightforward. The decision to move elements or to coarsen is not as easy. Coarsening implies that the solution does not need as much resolution as it has. While the spectrum decay predicts convergence if one adds resolution, it does not have the ability to predict convergence if one removes resolution. Theoretically, one might be able to look at the level of the spectrum coefficients and estimate what error would be incurred by removing the last coefficient. However, this is not very robust, particularly in transient problems. For these reasons, coarsening is limited to moving elements. The criterion for moving elements again relies on comparing neighbouring elemental error estimates. However, it is difficult to write a democratic algorithm which does not destroy the mesh, by having too many elements changing at once. For this purpose, a voting system was implemented to mark elements with the grestest need for increased "resolution". The algorithm examines each element and its neighbours, compares their error estimates and accordingly votes for the element with the greatest error. After passing through the whole grid, a list of the elements with the greatest number of votes is obtained. At the same time, an indication of the relative error is saved to serve as a value for shrinking each marked element and to indicate from which neighbour the resolution may be taken. Again, a limit is imposed to prevent drastic size reductions at the expense of neighbouring elements. While the refinement option to move elements or grid reconstruction is attractive since it incurs no extra cost, it is the most difficult to implement. In two and three dimensions the difficulties increase.

As mentioned above, the decay rate σ of the spectrum of each element is used as a refinement criterion to opt between increasing the order of the polynomial, N, and increasing the number of elements, K. These are often referred to in the finite element community as p- and h-refinement respectively [e.g. 7] and are similar in the spectral element method.

2.3 Refinement Process

Once the elements have been marked for refinement and all the limits and tolerances have been checked, the refinement process proceeds. There are three types of refinement.

1) For mesh reconstruction or zero-cost refinement by moving elements and adjusting their relative sizes, the elements with the most votes for refinement are shrunk in size according to their relative errors with their neighbours. The extra space released by the shrinking of the

element is added to the neighbour element, keeping the total space constant. An algorithm is implemented to check that the entire domain has been covered and that there are no holes in the grid.

2) For refinement by increasing the order of the polynomial N, the order is simply increased by two to N+2.

3) For refinement by increasing the number of elements K, the element to be refined is simply split in two and the polynomial is decreased by two to N-2, with a lower limit imposed on the order. The reduction in polynomial order is introduced since the decay rate has shown that an Nth order polynomial is not resolving the solution well and is therefore wasteful.

In two and three dimensions, error estimates and decay rates are obtained for each direction in each element and hence the adaptive refinement decisions may be carried out in each direction. At all times in the process, the aim is to use the minimum amount of resolution to obtain the best solution possible. In the interest of efficiency, there is no "backtracking" to improve the solution. Since the problems to be treated are transient this necessitates a tolerance to be imposed at all times. The error estimates may be calculated at every step to ensure the tolerance is imposed but this can be expensive. Instead, errors are checked periodically with a frequency imposed by the user. Since increase in resolution is also expensive, necessitating a recalculation of the discrete operator matrix, adaptivity is also done only periodically with a frequency imposed by the user. In practice, the no-cost refinement of moving the elements is allowed more often than the true refinement procedures of increasing N or K.

3. Illustrations

3.1 Burgers' Equation

The one-dimensional viscous Burgers equation

$$\frac{\partial u}{\partial t} + u\frac{\partial u}{\partial x} = \nu\frac{\partial^2 u}{\partial x^2}, \quad x \in [-1; 1], \quad t \geq 0 \tag{4a}$$

with boundary conditions

$$u(-1,t) = u(1,t) = 0 \tag{4b}$$

and initial conditions

$$u(x,0) = -\sin\pi x \tag{4c}$$

was chosen to illustrate the capabilities of the adaptive method. For low viscosities, this equation admits a nonsingular thin internal boundary layer that must be resolved for spatially and temporally accurate numerical solutions to be obtained. An analytical solution is available [8,9] and is used to determine accuracy. For $\nu = 0.01/\pi$ the solution develops a sharp gradient at the origin at approximately $t = 1/\pi$. The gradient reaches a maximum at approximately $t = 0.5$. A full study of this equation by several different spectral methods was reported in [10]. The conclusion of that study was that spectral methods were not well suited to the calculation of thin inner layers. This is especially true if the location of the layers are unknown. The study found that accurate results could be obtained but polynomial orders were inordinately high for this simple one-dimensional problem. The best spectral method required N=64 for three digit accuracy, while the spectral element method obtained four digit accuracy with N=16 and K=4.

Further, the time step needed to accurately model this transient process was very small due to stability restrictions. The present results show that spectral methods are indeed well suited to these types of problems provided adaptivity is performed.

Discretization

We begin with the temporal discretization. The nonlinear convective term of Burgers' equation is treated explicitly via a third order Adams-Bashforth technique which is stable for Courant numbers less than 0.72. The diffusion term is evaluated implicitly via Crank-Nicolson, which is unconditionally stable. The time stepping is done in two steps:

$$\frac{\hat{u} - u^n}{\Delta t} = -\frac{1}{2} \sum_{q=0}^{2} \alpha_q \frac{\partial (u^{n-q})^2}{\partial x} \tag{5a}$$

$$\frac{u^{n+1} - \hat{u}}{\Delta t} = \nu \frac{\partial^2 (\frac{u^{n+1}+u^n}{2})}{\partial x^2} \tag{5b}$$

where the α_q are the third order Adams-Bashforth coefficients

$$\alpha_0 = \frac{23}{12} \quad \alpha_1 = -\frac{4}{3} \quad \alpha_2 = \frac{5}{12}. \tag{5c}$$

The spatial discretization follows the standard spectral element formulation [e.g. 4,10,11], hence it is only described briefly. The spectral element method breaks up the computational domain into k=1,K macro-elements of lengths L^k, upon each of which the unknown u is expanded as a Lagrangian interpolant through the Gauss-Lobatto collocation points:

$$u^k(r) = \sum_{i=0}^{N} u_i^k h_i(r) \tag{6}$$

where u_i^k is the value of the unknown on element k at the collocation point r_i. The interpolants are given by

$$h_i(r) = \frac{(r^2 - 1)P_N'(r)}{N(N+1)(r - r_i)P_N(r_i)} \quad r \in [-1; 1]. \tag{7}$$

Here, P_N is the Nth order Legendre polynomial. The collocation points, r_i, are the zeroes of the numerator in Equation (7). Each element is mapped to the interval $[-1; 1]$. The discrete solution may also be expressed in terms of the spectrum a_n as in Equation (1). The equations are written in a variational formulation and all integrals are performed by Gauss-Lobatto Legendre quadrature.

Results

The viscous Burgers equation is solved for three cases. For a low viscosity, $\nu = 0.01/\pi$, the equation exhibits a sharp gradient as illustrated in Figure 1a by the spectral element solution using N=15 and K=4. This solution has four digit accuracy in the maximum gradient at the origin as shown in Table 1, where it is compared with the analytical and other non-adaptive spectral element solutions. This case is used to illustrate the power of the adaptive method to refine sharp gradients. For high viscosity, $\nu = 1/4\pi$, the diffusion terms dominate and the gradient is weak, as shown in Figure 1b. This case illustrates how the adaptive method

5

behaves in a problem where gradients are weak. The third case involves the solution to Burgers' equation (4) with a new initial condition $u = -\sin\pi x + 0.5$ and periodic boundary conditions. The solution to this problem is a steepening wave travelling towards $x = 1$ shown in Figure 2. This case illustrates how the adaptive method can resolve non-stationary fronts.

In each case, the figures show the time evolution of the solution u to Equation (1) and the grid used. The grid, represented by symbols, is denoted by the element boundaries ($|$) and the collocation points inside each element ($\star$). Each grid is plotted once when it is newly implemented at a vertical axis coordinate corresponding to time $-t$ in Equation (4), except where noted.

  1) $\nu = 0.01/\pi$

Several properties of the method are illustrated. Each type of refinement will be studied separately and the combined adaptive result is shown.

The first test case, illustrated in Figure 3, shows the merit of refining away from the sharp gradients. In Figure 3a, we show a solution where there is sufficient resolution around the sharp gradient (N=11 in two elements of size $\Delta x = 0.05$ around the origin) but poor resolution away from the thin layer (N=3 in four elements of size $\Delta x = .475$). Note that the initial condition is sufficiently resolved, but as time evolves, errors become significant. The error in the gradient is small but the error in time is significant. In Figure 3b, we present the adaptive solution starting with the same initial resolution. By adaptively refining the smooth regions by increasing the order of the polynomial from N=3 to N=7 at t=0.1, the errors are reduced significantly. The error estimates indicate an error of 10^{-3} before refinement and 10^{-5} thereafter.

The second test case, illustrated in Figure 4, shows the merit of no-cost refinement by adapting the size and position of elements. In Figure 4a, we show a high resolution solution (N=11, K=4) but with non-optimal equally spaced elements. Note that resolution is adequate up until approximately $t = 0.3$. Beyond, a large oscillation appears indicating poor resolution around the sharp gradient. The temporal error is moderate but the error in the maximum gradient is significant. In Figure 4b, we present the adaptive solution starting with the same initial resolution. By checking every $\Delta t_\in = 0.5$ and adaptively refining by shrinking the elements with the greatest errors, we obtain a significantly improved solution. Note that refinement, does not start until $t = 0.25$ as it is not needed until then. At $t = 0.45$, shortly before the maximum gradient develops, the finest grid is chosen with the smallest elements around the sharp gradient of size $\Delta x = 0.03125$. The tolerance for the error estimates is 10^{-4}. Again the errors in the maximum gradient and time at which it occurs are significantly reduced.

The third test case, illustrated in Figure 5, shows the merit of refining by increasing the number of elements. In this case, we choose to illustrate the point with a poor resolution run. In Figure 5a, we show a low resolution run with N=3 and K=4. The initial grid consists of equally spaced elements. We adaptively refine by moving elements only (no-cost refinement). Despite clustering small elements near the sharp gradient, the errors remain large. Note the large overshoots. This case shows that refinement by adjusting element sizes is not sufficient for improved solutions. In Figure 5b, we show a solution with the same initial grid, where refinement has been adaptively performed by increasing the number of elements only. By checking the error estimates every $\Delta t_K = 0.1$ and adding elements each time since the errors were poor throughout, the adaptive method obtains a vastly improved solution. The final grid has K=14 elements and a fixed N=3 per element. The error in the maximum gradient is improved from a 66% error to an 11% error. The error in the time at which the maximum gradient occurs is also significantly improved. As the errors are still large, it is obvious that

none of these refinement methods is optimal. The best refinement procedure combines all three as illustrated in the following case.

The fourth test case is a fully adaptive case where all three refinement methods are used. In Figure 6, the time evolution of the solution and of the grid is presented. The element demarcations (|) are not shown for clarity. This case was obtained with a frequency of adaptivity in element size of $\Delta t_\epsilon = 0.03$, in N of $\Delta t_N = 0.075$, and in K of $\Delta t_K = 0.075$, an absolute tolerance on the error estimators of 5.10^{-5}, a relative tolerance of 5, a maximum on N of 11 and a maximum on K of 20, a minimum element size of $\Delta x = 0.01$ and a minimum time step size of 10^{-4}. The initial grid is a relatively coarse K=4 equally spaced elements with N=5 in each. The final grid has K=16 elements with polynomial orders ranging from N=5 to N=9. The low order N=5 elements are generally in the edge areas of the sharp jump and away from the jump, while high order polynomials are used in the smooth regions of the jump. Since this is a viscous phenomenon, the jump is not a discontinuity but rather a thin layer. Hence it is expected that the adaptive algorithm would refine in this way. There are many possibilities for an adaptive solution. The choice of adaptivity frequency, absolute and relative tolerances, minimum and maximum resolution are left to the user. The results show excellent resolution. The maximum gradient is captured with five significant digits and the time at which it occurs is accurate to within the smallest time step size used ($\Delta t_{min} = 0.0005$). Comparing with the non-adaptive solutions of Table 1 we see that the solution is better than the corresponding N=17 K=4 non-adaptive solution. The greatest expense in a spectral element solution is related to the storage (if a direct inversion method is used) and the inversion of the discrete operator matrix. The amount of work scales linearly with the number of elements and nonlinearly with the polynomial order. Hence the savings afforded by being able to use more elements and lower order polynomials is substantial because the bandwidth of the matrix is greatly reduced. In this example, the maximum amount of work per iteration presents a savings of 22%. But the real savings is associated with the transiently adapting solution. Where the solution has not yet developed any fine structures, a coarse grid and a large time step can be used. Including these, the savings is of 37% for this example.

2) $\nu = 1/4\pi$

For this high viscosity case, the solution exhibits only weak gradients as illustrated in Figure 1b. We present only one test case, illustrated in Figure 7, to show how the adaptive method handles weak gradients. The initial grid has K=4 equal spaced elements with N=5 on each. As expected, the adaptive method refines by increasing the order of the polynomial and by adjusting element sizes. The error estimators never indicate poor decay rates since this is a smooth solution which is ideal for spectral discretization. Hence no elements are ever added in the adaptive refinement process. The number of elements remains at K=4 while the polynomial order is increased from N=5 to N=7 in the regions of the weak gradient. Note that very little resolution is needed in comparison to the sharp gradient case.

3) Moving Front

The challenge of the moving front case is to track the steepening wave with sufficient resolution, without wasting resolution in areas where the wave has passed through. This case therefore depends on a good coarsening algorithm. The results are presented in Figure 8. Again, element demarcations (|) are not shown for clarity. The adaptive method accurately resolves the steepening moving front. This case has an initial grid of K=4 equally spaced elements and N=7 on each element. The final grid has K=7 elements with polynomial orders ranging from 7 to 19. As mentioned above, coarsening is difficult to do without losing accuracy. Coarsening is

7

limited to element size and position changes. As a result, the coarsening is somewhat inefficient in this case. This is due to the fact that the sharp gradient is adaptively resolved by many small elements and that moving these small elements relative to each other is a slow process for coarsening. However, the adaptive method successfully tracks the moving front and coarsens in the regions behind it once it has moved away.

The three test cases on Burgers equation show the capabilities of the adaptive method to optimally refine solutions in common situations. We now turn to two-dimensional problems where adaptivity becomes more complex, but where potential savings increase dramatically.

3.2 Driven Cavity Flow

Laminar two-dimensional flow in a cavity is used to illustrate how the adaptive process performs in higher dimensions. The full incompressible Navier-Stokes equations

$$\frac{\partial \vec{u}}{\partial t} + \vec{u} \cdot \nabla \vec{u} = -\nabla p + \frac{1}{R} \nabla^2 \vec{u} \tag{8a}$$

$$\nabla \cdot \vec{u} = 0, \tag{8b}$$

where $\vec{u}$ is the velocity vector, p is the pressure and R is the Reynolds number, are solved in a geometry shown in Figure 9. The flow in the cavity is driven from above with a uniform unit velocity. The boundary conditions are all Dirichlet: $u = 1$, $v = 0$ at $y = 1$ and no-slip boundary conditions on the three walls of the cavity $y = 0$, $x = 0$ and $x = 1$. This flow is a popular test case; some references are given in [13]. The discontinuity in velocity at the upper corners, where $u = 0$ from the no-slip condition and $u = 1$ from the imposed driving flow, can present problems in the numerical solution. At these points there is a singularity as the vorticity becomes infinite. A priori, since the location of the singularity is known, one can resolve it adequately in an initial grid. However, the location of singularities is not always known and the optimal degree and type of resolution is not known. This example will illustrate how the adaptive method refines singularities in a general way. Further, as savings in cpu and storage become more important in two and three dimensions, adaptive refinement in two and higher dimensions is imperative. The nonconforming spectral element formulation provides the ability to locally refine without incurring undue increase in resolution globally. The automation of the adaptation greatly enhances the advantages of the nonconforming method as illustrated in this example.

Discretization

The Navier-Stokes equations (8) are advanced in time using an explicit/implicit fractional time-stepping scheme [1,12], which results in a set of separate equations for p and $\vec{u}$. The nonlinear terms are treated explicitly as a simple inhomogeneity in the elliptic equation set. The spatial discretization is a nonconforming spectral element method described in [5]. Here, we briefly review the nonconforming formulation.

The nonconforming discretization allows arbitrary element matchups in the computational grid, an example of which is shown in Figure 10b. While C^0 continuity is lost due to the mismatch of approximating polynomials on either side of an elemental interface, the consistency error is held as small as the approximation errors, thereby preserving the convergence properties of the spectral element discretization. The implementation consists of introducing a new structure known as mortars γ^p, which are defined as the intersection of adjacent element edges.

Upon this structure, ϕ is defined as the mortar function, which is a polynomial of degree N in the local one-dimensional mortar variable s. The approximation space X_h consists of the functions v in $\mathcal{L}^2$ that are tensor products of polynomials of degree N in each direction of each element k, such that the two following conditions are satisfied:

1- the vertex condition: at each vertex q of each element k, $v_{|_k}(q) = \phi(q)$.

2- the $\mathcal{L}^2$ condition: over each elemental edge, $\forall \psi \in P_{N-2}$ $\int_{edge}(v - \phi)\psi ds = 0$.

For a conforming approximation this definition of X_h reduces to the standard spectral element approximation space. The vertex condition ensures exact continuity at cross points while the $\mathcal{L}^2$ condition represents a $\mathcal{L}^2$ minimization of the jump in functions at internal boundaries. The combination of these two conditions ensures the optimality of the discretization, as explained and illustrated in [5].

Results

The driven cavity flow is solved adaptively starting with a coarse N=4 K=4 equal-sized element grid shown in Figure 10a. In each figure, the grid is shown by solid element boundary lines. The collocation points are not shown. The Reynolds number for this test case is R=100. The streamlines are shown for purposes of comparison. In this test case, refinement is limited to moving elements, splitting elements and increasing the polynomial order globally. The option to increase order locally is not used. For this steady-state problem, adaptivity in time is not crucial. Figure 10 presents the intermediate adaptation steps. The first adaptation (Figure 10b) subdivides the upper corner elements into four as both x and y direction decay rates are below 1. The number of elements grows from K=4 to K=10. The second adaptation (Figure 10c) shrinks the corner elements at the expense of their neighbours. This is a no-cost refinement step which decreases errors only slightly. The third adaptation (not shown) increases the order of the polynomial globally to N=6. The fourth adaptation (Figure 10d) subdivides the corner elements in the y direction. The number of elements grows from K=10 to K=12, while the polynomial order remains N=6 from the previous step. Because the singularity is difficult to resolve with smooth polynomials, the error estimator always indicates poor decay rates in the elements containing the singularities. Hence, refinement by adding or splitting elements is dominant in this case. In two dimensions, as in one, the error estimators perform very well. The decay rate is measured in both x and y directions, providing adaptivity criteria for both directions. In adapting from the mesh in Figure 10c to that in Figure 10d for example, the decay rate is below 1 only in the y direction for the corner elements; hence adaptivity proceeds by splitting the corner elements vertically only. The error estimates are reduced from 10^{-1} to 10^{-4} in most of the domain. In the corner elements containing the singularities, the error estimates are reduced to 10^{-2}. These relatively poor errors are expected as the singularity is hard to resolve with smooth functions. Further refinement could reduce this error. However, the main advantage of the adaptive method is demonstrated: the error due to the singularity is localized to a very small element and contamination of the rest of the domain is minimized.

4. Conclusions

The test cases presented clearly show that the adaptive formulation of the spectral element method increases the flexibility and capabilities of the method. Sharp gradients, singularities and regions of poor resolution can be resolved optimally. The method combines three types of

9

refinement using criteria based on error estimators which indicate the quality of the resolution on each element. The savings in storage and cpu time appear to be considerable. In two and three dimensions the savings increase. The increase in efficiency should broaden the range of problems that can be investigated by high order spectral type methods. Generally, the savings is afforded by using a larger number of elements, with very high order only in elements where it is really needed and effective. These are regions of smooth solutions. In regions of discontinuities or sharp structures many lower order elements are used. A larger number of elements can also increase the efficiency of coarse-grained parallel implementation of the method [14], since a larger number of elements can be distributed among many processors. The overhead associated with adaptivity, however, can be substantial. The error estimators are relatively cheap to calculate but the inversion of the matrix that is needed with each new grid is expensive. This expense is minimized by adapting only periodically. While the refinement capabilities were successfully demonstrated here, the coarsening algorithm remains somewhat inefficient. A more clever algorithm will be the subject of future work.

This study of the practical aspects of adaptive meshes serves as a learning step in the ongoing development of a fully automatic adaptive mesh procedure for spectral element methods in two and three dimensions. The purpose of this work is to make high order spectral methods more accessible to engineers for the simulation of complex physical phenomena by automating the grid generation and refinement processes and by reducing resolution requirements significantly.

References

[1] S.A. Orszag and L.C. Kells – Transition to turbulence in plane Poiseuille and plane Couette flow, *Journal of Fluid Mechanics*, **96** (1980), p. 159.

[2] S.A. Orszag and A.T. Patera – Secondary instability of wall-bounded shear flows, *Journal of Fluid Mechanics*, **128** (1983), p. 347.

[3] D. Gottlieb and S.A. Orszag – *Numerical Analysis of Spectral Methods: Theory and Applications*, SIAM, Philadelphia (1977).

[4] A.T. Patera – A spectral element method for fluid dynamics: Laminar flow in a channel expansion, *Journal of Computational Physics*, **54** (1984), p.468.

[5] Y. Maday, C. Mavriplis, A. T. Patera – Non-conforming mortar element methods: application to spectral discretizations, *Domain Decomposition Methods*, SIAM, Philadelphia (1989), p. 392.

[6] C. Mavriplis – A posteriori error estimators for adaptive spectral element techniques, *Notes on Numerical Fluid Mechanics*, Vol. 29, Vieweg (1990), p. 333.

[7] P. Devloo, J. T. Oden, P. Pattani – An h-p adaptive finite element method for the numerical simulation of compressible flow, *Computer Methods in Applied Mechanics and Engineering*, **70** (1988), p. 203.

[8] J.D. Cole – On a quasi-linear parabolic equation occurring in aerodynamics, *Quarterly of Applied Mathematics*, **9** (1951), p. 225.

[9] E.R. Benton and G.N. Platzmann – A table of solutions of one-dimensional Burgers equation, *Quarterly of Applied Mathematics*, **29** (1972), p. 195.

[10] C. Basdevant, M. Deville, P. Haldenwang, J.M. Lacroix, J. Ouazzani, R. Peyret, P. Orlandi and A.T. Patera – Spectral and finite difference solutions of the Burgers equation, *Computers and Fluids*, **14**, 1 (1986), p. 23.

Method	$\left|\frac{\partial u}{\partial x}\right|$max	$t_{\max}$
Non-Adaptive N=5	167.227	0.53745
Non-Adaptive N=7	167.449	0.50848
Non-Adaptive N=9	154.019	0.50611
Non-Adaptive N=11	150.812	0.51071
Non-Adaptive N=13	151.496	0.51103
Non-Adaptive N=15	151.977	0.51039
Non-Adaptive N=17	152.076	0.51071
Non-Adaptive N=19	151.991	0.51023
Non-Adaptive N=21	152.004	0.51023
Adaptive (Case 4)	152.022	0.51028
Analytical	152.00516	0.51047

Table 1: Maximum absolute value of the slope at the origin and time at which it occurs for the non-adaptive and adaptive spectral element and analytical solutions to Burgers equation with $\nu = 0.01/\pi$

[11] Y. Maday and A.T. Patera — Spectral element methods for the Navier-Stokes equations, in A.K. Noor, editor, *State-of-the-Art Surveys in Computational Mechanics*, ASME, New York (1988).

[12] G.E. Karniadakis — Spectral element simulations of laminar and turbulent flows in complex geometries, *Applied Numerical Mathematics*, 6 (1989/90), p. 85.

[13] R. Peyret and T.D. Taylor — *Computational Methods for Fluid Flow*, Springer, New York (1983).

[14] P.F. Fischer, L.W. Ho, G.E. Karniadakis, E.M. Ronquist and A.T. Patera — Recent advances in parallel spectral element simulation of unsteady incompressible flows, *Proceedings of the Symposium on Advances and Trends in Computational Structural Mechanics and Computational Fluid Dynamics, Washington, DC* (1988).
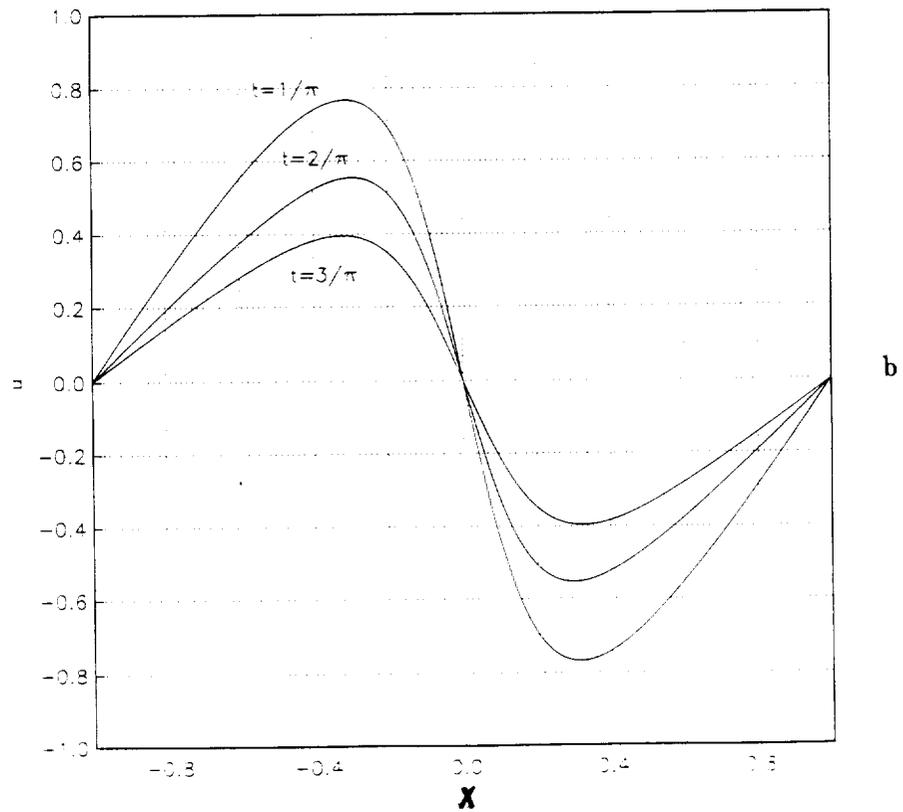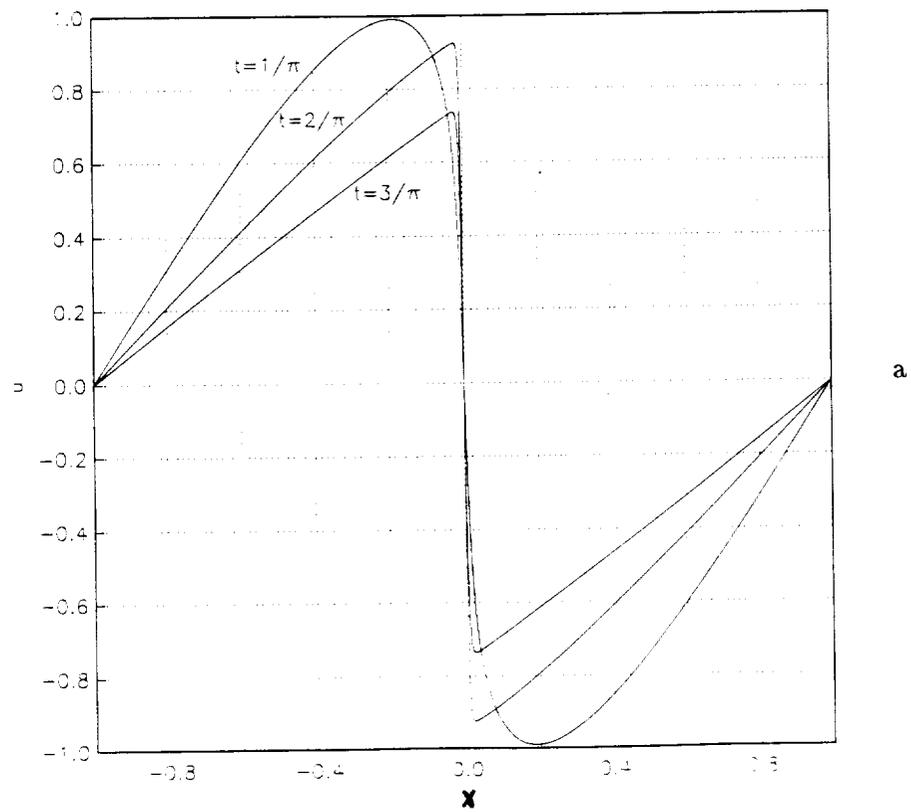
Figure 1: Time evolution of the solution to the viscous Burgers equation with homogeneous bounday conditions and sine wave initial condition a) low viscosity $\nu = 0.01/\pi$ sharp gradient case b) high viscosity $\nu = 1/4\pi$ weak gradient case
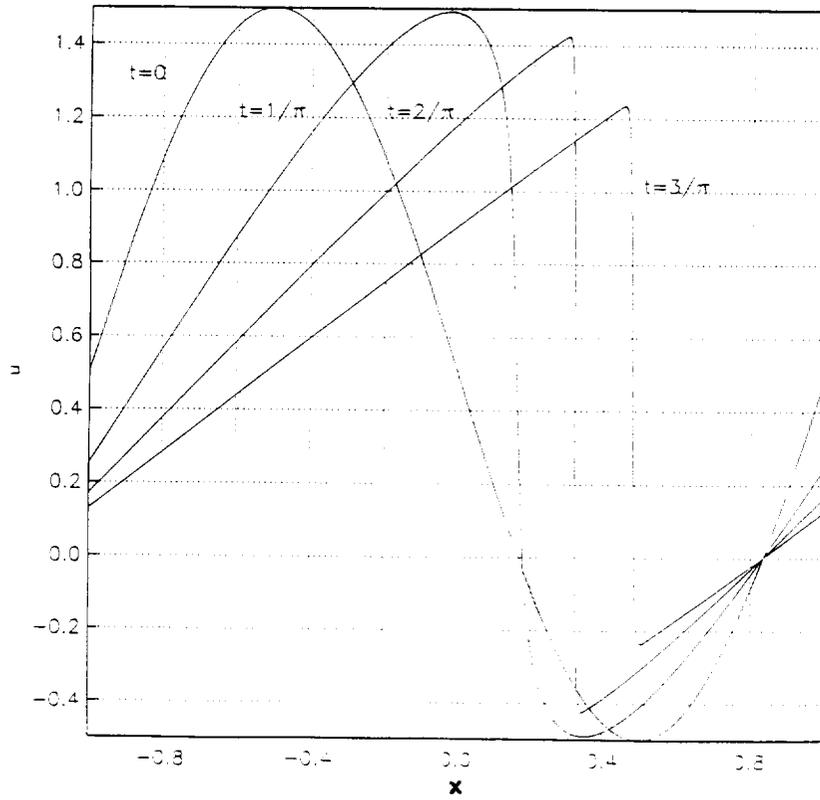
Figure 2: Time evolution of the solution to the viscous Burgers equation with $\nu = 0.01/\pi$, periodic boundary conditions and initial condition of a $\sin(\pi x) + 0.5$
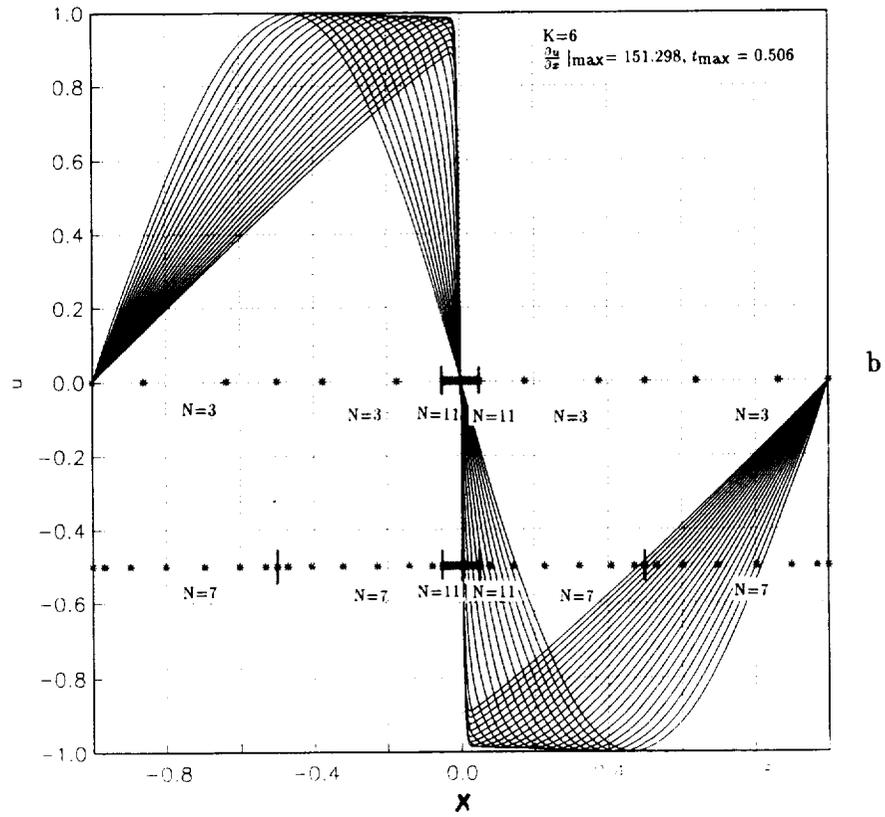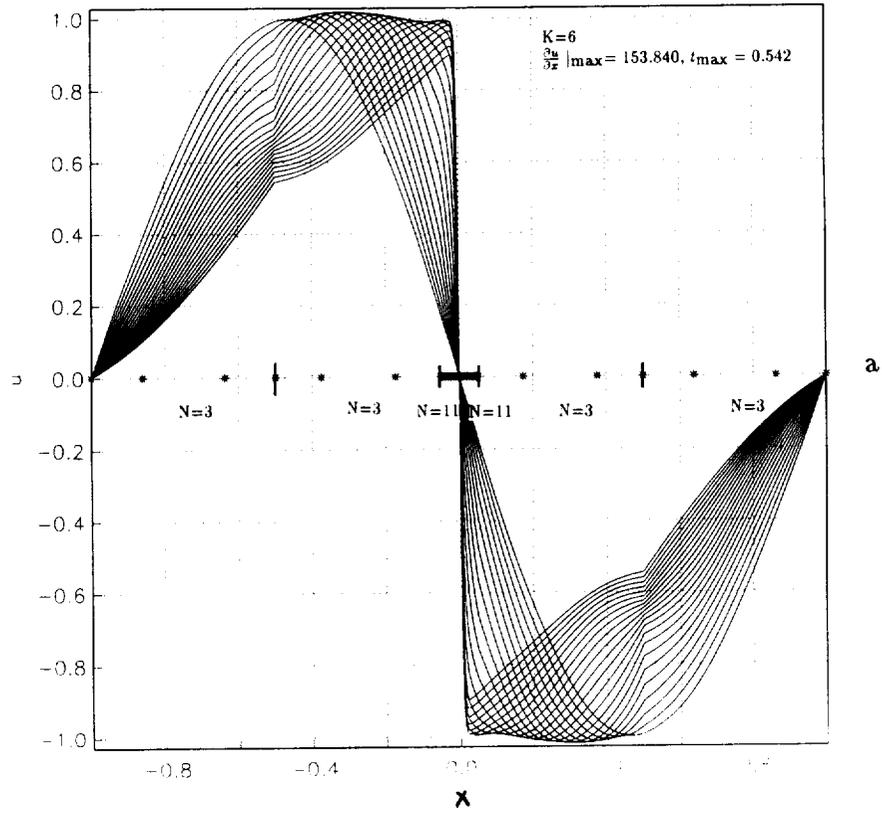
Figure 3: Effect of refinement by increasing polynomial order in smooth regions of the solution to the viscous Burgers equation for low viscosities: a) fixed resolution solution b)increased resolution solution
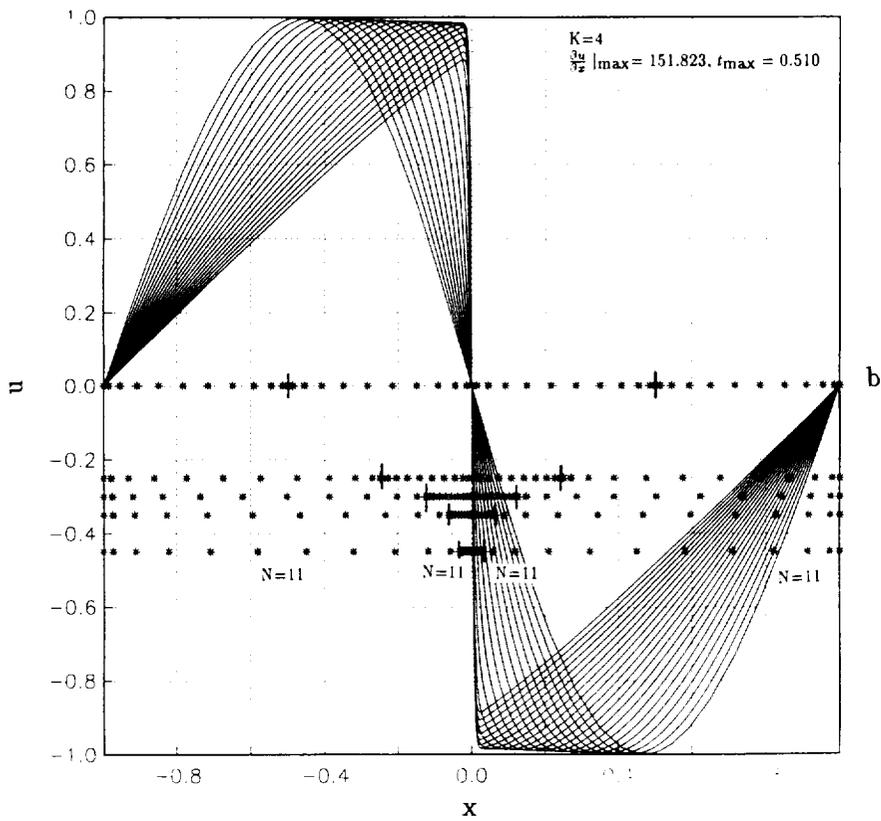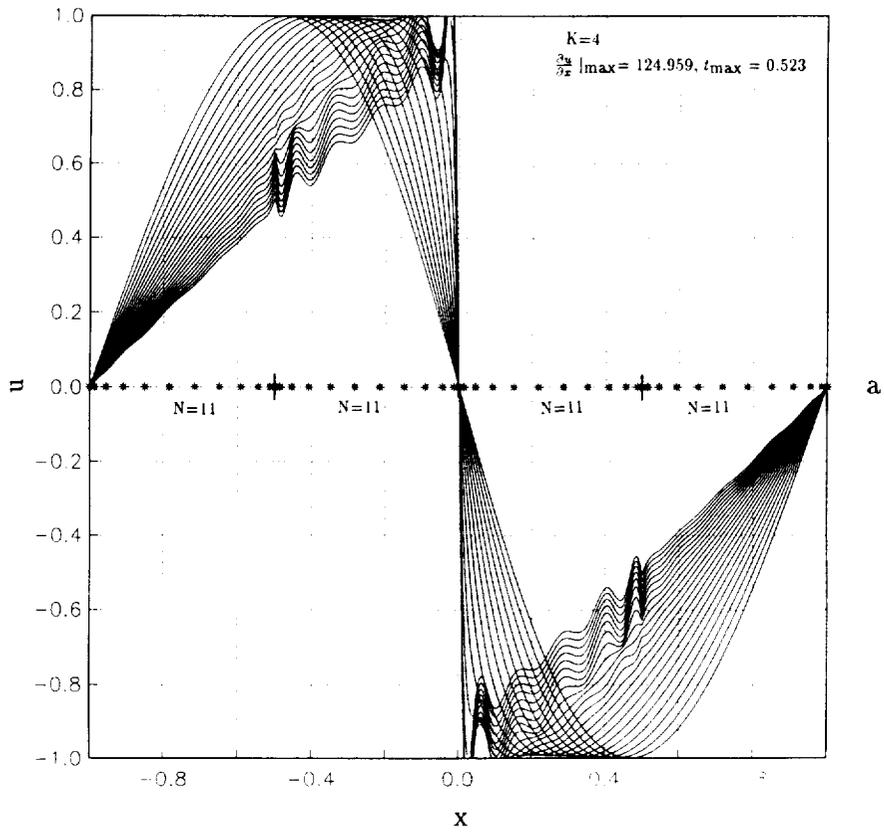
Figure 4: Effect of no-cost refinement by adapting element size and position for the solution to viscous Burgers equation for low viscosities a) fixed equally-spaced element solution b) adaptive solution
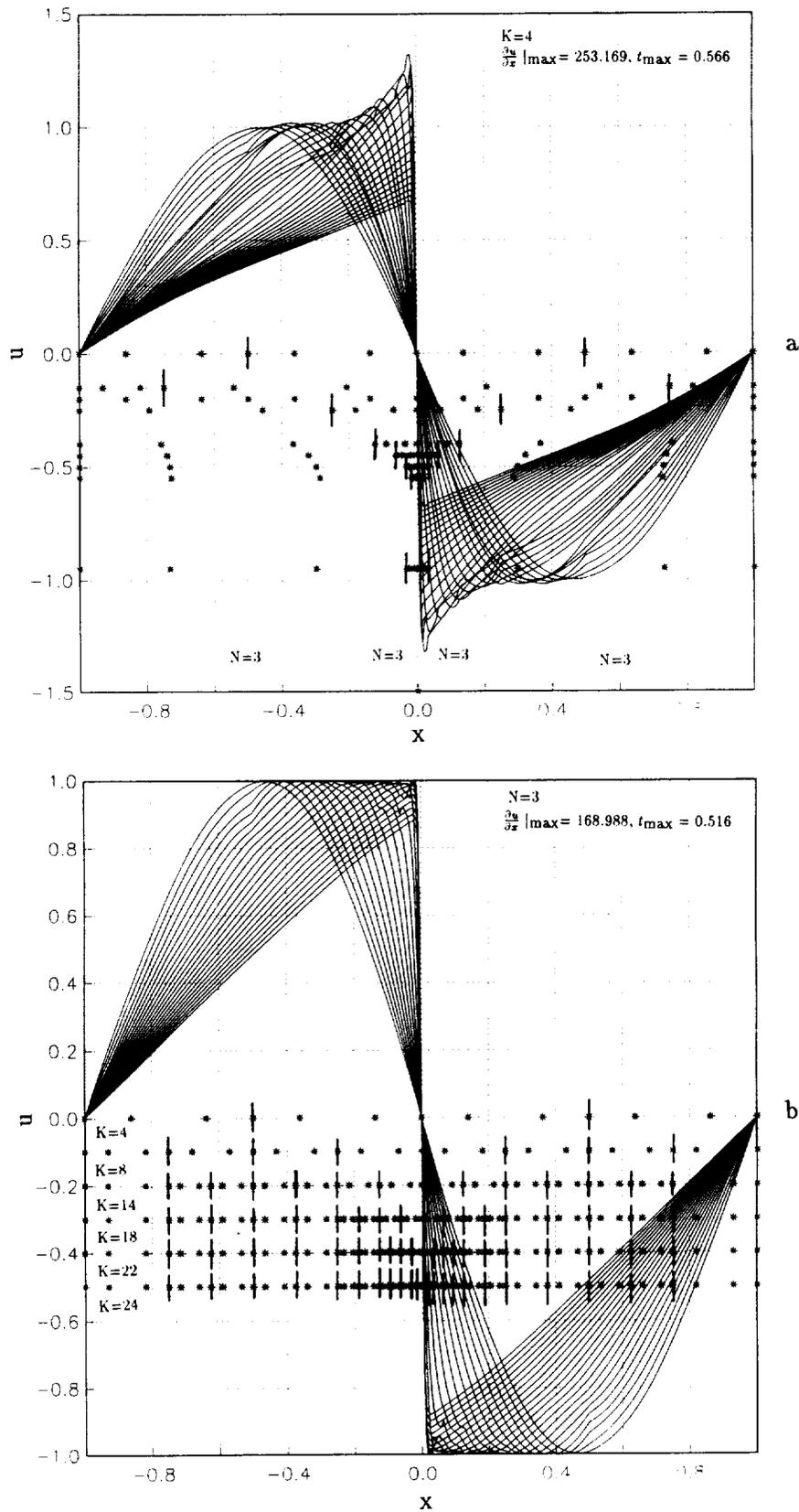
Figure 5: Effect of refinement by adapting increasing the number of elements for the solution to viscous Burgers equation for low viscosities a) fixed low order but adaptive element size solution b) adaptive (number of elements) solution

$\frac{\partial u}{\partial x}|_{\max} = 152.022, t_{\max} = 0.510277$
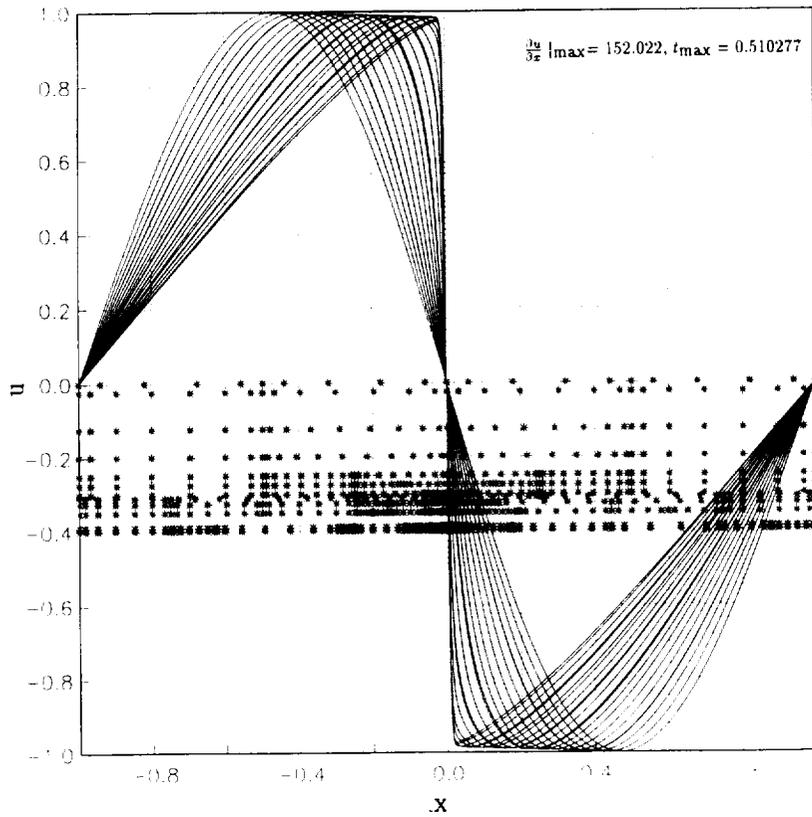
Figure 6: Fully adaptive solution to viscous Burgers equation for low viscosities: final grid has K=16 and N varying from 5 around the leading and trailing edges of the sharp jump to N=9 within the jump
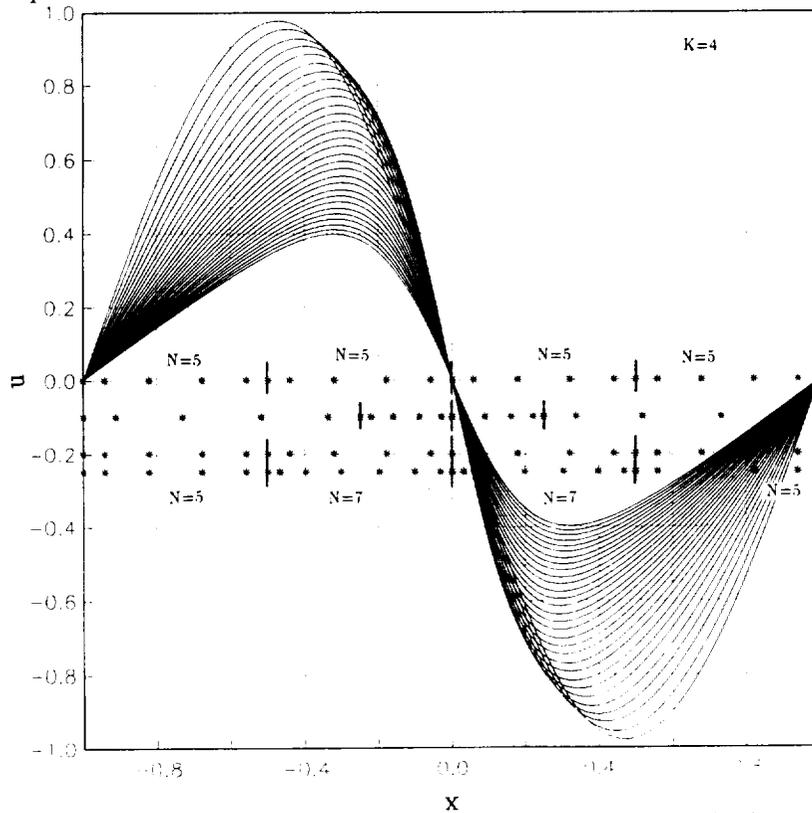

Figure 7: Fully adaptive solution to viscous Burgers equation for high viscosity: $\nu = 1/4\pi$

17
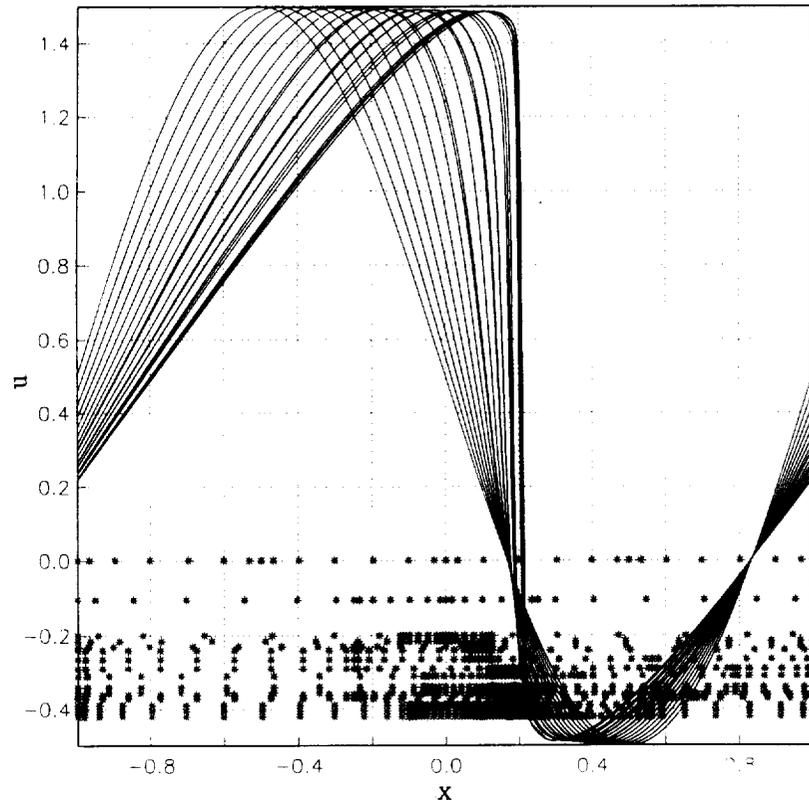
Figure 8: Fully adaptive solution to viscous Burgers equation for moving front case: both refinement and coarsening are used
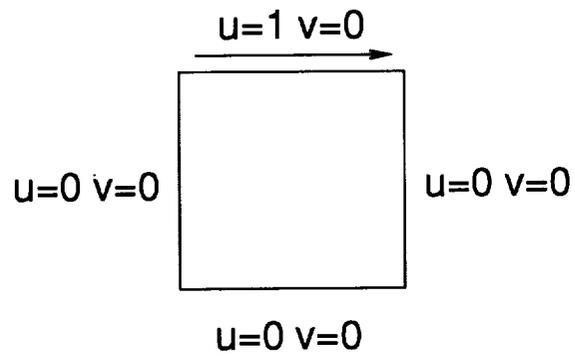
Figure 9: Geometry for two-dimensional Navier-Stokes fluid flow in a driven cavity
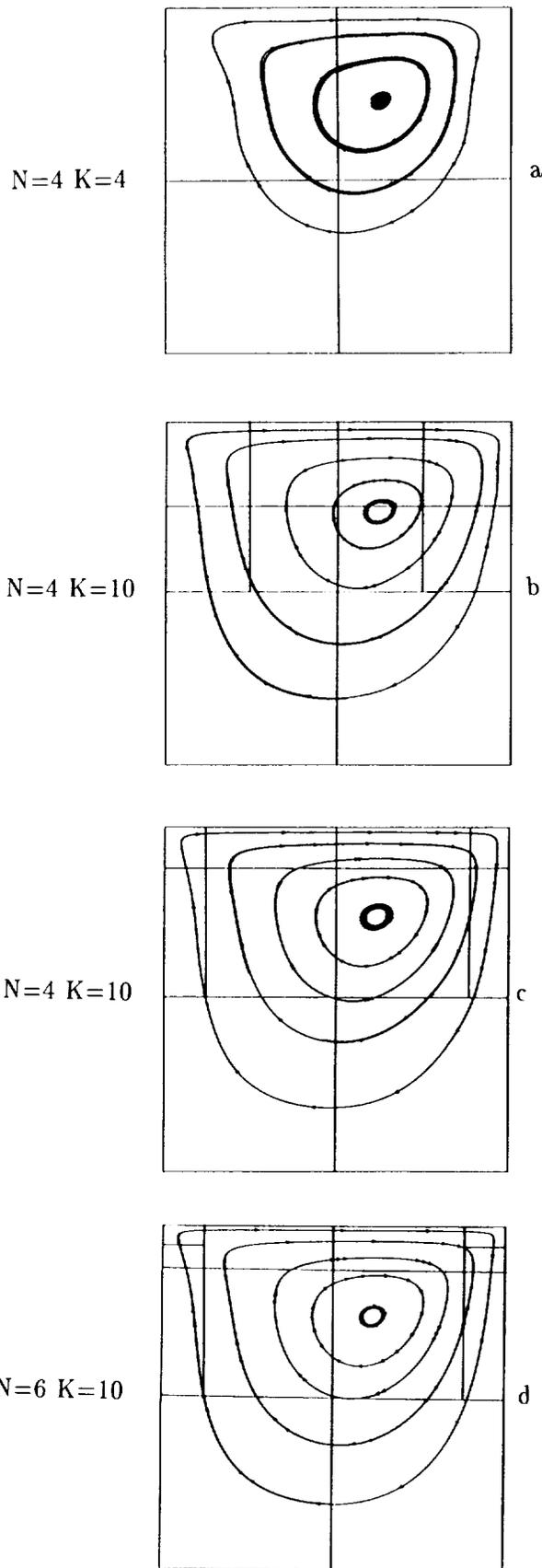
Figure 10: Adaptive solution to the two-dimensional Navier-Stokes equations for fluid flow in a driven cavity represented by streamlines: a) initial coarse grid b)-d) intermediate adaptive grids

REPORT DOCUMENTATION PAGE

Public reporting burden for this collection of information is estimated to average 1 hour per response, including the time for reviewing instructions, searching existing data sources, gathering and maintaining the data needed, and completing and reviewing the collection of information. Send comments regarding this burden estimate or any other aspect of this collection of information, including suggestions for reducing this burden to Washington Headquarters Services, Directorate for Information Operations and Reports, 1215 Jefferson Davis Highway, Suite 1204, Arlington, VA 22202-4302, and to the Office of Management and Budget, Paperwork Reduction Project (0704-0188), Washington, DC 20503.

1. AGENCY USE ONLY (Leave blank)	2. REPORT DATE July 1992	3. REPORT TYPE AND DATES COVERED Contractor Report

4. TITLE AND SUBTITLE

ADAPTIVE MESH STRATEGIES FOR THE SPECTRAL ELEMENT METHOD

5. FUNDING NUMBERS

C NAS1-19480

WU 505-90-52-01

6. AUTHOR(S)

Catherine Mavriplis

7. PERFORMING ORGANIZATION NAME(S) AND ADDRESS(ES)

Institute for Computer Applications in Science
  and Engineering
Mail Stop 132C, NASA Langley Research Center
Hampton, VA 23665-5225

8. PERFORMING ORGANIZATION REPORT NUMBER

ICASE Report No. 92-36

9. SPONSORING / MONITORING AGENCY NAME(S) AND ADDRESS(ES)

National Aeronautics and Space Administration
Langley Research Center
Hampton, VA 23665-5225

10. SPONSORING / MONITORING AGENCY REPORT NUMBER

NASA CR-189686
ICASE Report No. 92-36

11. SUPPLEMENTARY NOTES

Langley Technical Monitor: Michael F. Card
Final Report

Submitted to Proc. of ICOSAHOM
'92 Conf.; To appear in the
Journal "Comp. Methods in Appl.
Mechanics and Engineering"

12a. DISTRIBUTION / AVAILABILITY STATEMENT

Unclassified - Unlimited

Subject Category 34, 64

12b. DISTRIBUTION CODE

13. ABSTRACT (Maximum 200 words)

An adaptive spectral element method has been developed for the efficient solution
of time dependent partial differential equations. Adaptive mesh strategies that in-
clude resolution refinement and coarsening by three different methods are illustrated
on solutions to the one-dimensional viscous Burgers equation and the two-dimensional
Navier-Stokes equations for driven flow in a cavity. Sharp gradients, singularities
and regions of poor resolution are resolved optimally as they develop in time using
error estimators which indicate the choice of refinement to be used. The adaptive
formulation presents significant increases in efficiency, flexibility and general
capabilities for high order spectral methods.

14. SUBJECT TERMS

spectral methods; adaptive

15. NUMBER OF PAGES

21

16. PRICE CODE

A03

17. SECURITY CLASSIFICATION OF REPORT	18. SECURITY CLASSIFICATION OF THIS PAGE	19. SECURITY CLASSIFICATION OF ABSTRACT	20. LIMITATION OF ABSTRACT
Unclassified	Unclassified		

NSN 7540-01-280-5500